JOURNAL OF MATERIALS SCIENCE 35 (2000) 4589–4600

Incorporation of the heating effect of the light source in a non-isothermal model of a visible-light-cured resin composite

D. PANANAKIS, D. C. WATTS
University of Manchester Dental School, Biomaterials Science Unit, Manchester, M15 6FH, UK
E-mail: dimitrios.pananakis@man.ac.uk; david.watts@man.ac.uk

Recent non-isothermal reaction rate models of light cured resins presented by various researchers do not take into account the increase of the temperature due to the absorption and scattering of light energy within the resin. However, the reaction rate is a strong function of temperature and hence all the calculations performed not adopting this factor are not revealing the true characteristics of the cure process. In this work, the heating effect of the light source is calculated from simple DSC measurements commonly performed after the initial cure of the specimens is recorded. An additional deconvolution procedure of these irradiant heat flow measurements is also presented as well as numerical results from a simple two dimensional model illustrating the differences that result from the inclusion of this parameter in the non-isothermal calculations.

1. Introduction

Reaction rate models have been formulated for the analysis of visible light cure reactions of resin composites. These have been of two types, namely mechanistic [1, 2] and phenomenological [3, 4]. The latter type of model is of particular importance to the analysis of the cure behaviour of visible-light-cured (VLC) resin composites as recent research work [5, 6] has illustrated their ability to replicate with great accuracy isothermal reaction rate experiments performed by means of Differential Scanning Calorimetry (DSC). Hence, by extracting the model parameters from simple isothermal and dynamic DSC experiments, these models are capable of predicting the temporal evolution of the reaction rate and the glass transition temperature under isothermal conditions.

However, their unique capabilities over the mechanistic models are fully revealed when these models are utilized to simulate the cure under non-isothermal conditions, which prevail during cure in a dental restoration. Once the reaction is initiated in a restoration cavity, the exothermic reactions taking place inside the composite raise the temperature throughout its volume. An additional "heat source" is created by the absorption and scattering of light energy within the volume of the composite. This creates temperature gradients between the tooth and the composite creating a flow of heat, or else, an energy (heat) transfer mechanism. Moreover, temperature gradients between the air and the composite surface provide another path of heat transfer towards the lower temperature region.

The problem of predicting the cure behaviour of a reacting volume of material which is subjected to non-isothermal conditions (ie. does not have a uniform temperature throughout its volume), is a combined heat transfer and cure prediction problem. A transient solution of this problem can be effected by combining the heat sources that are present in the reactive volume (exothermic reactions + irradiant heating arising from light absorption and scattering effects) whilst continuously evaluating the temperature field.

Despite its importance, the non-isothermal behaviour of the VLC resins and resin composites has so far been modelled by various researchers [5, 7–9] based only on the temperature variations produced by the exothermic reactions. In other words, the assumption imposed by these models is that the incident light source is not responsible for any temperature rises, or even for any change in the non-isothermal conditions during cure. It seemed therefore of interest to incorporate in the non-isothermal models the influence of this additional source of heat during the cure of VLC composites.

A distinction between the temperature rises produced during curing by the exothermic reactions and the curing light can be only achieved if the heat generation rate produced by the latter mechanism alone is known. Measurement of the temperature variations within the polymer volume during the application of light is not adequate to establish a complete phenomenological model capable of predicting the cure behaviour. To achieve this, the combined heat generation term in the heat balance equation (Equation 1, below) must be known.

The measurement of the heat generation rate produced by the light source can ideally be achieved by using a power compensated photo-DSC system, since

this apparatus directly measures heat flow. Hence, if a black body specimen is placed on the measuring furnace, the heat flow measurement would be directly proportional to that energy being absorbed by the specimen. This measurement has already been outlined by Fisher *et al.* [10], where a graphite disk was used as an approximate "black body" to provide a measure of the effective irradiance of the light source. In this investigation however, where the interest lies on the determination of heat absorbed by VLC dental composites, such a measurement using graphite disks would surely overestimate this parameter, as the surface reflectivity of the composite is greater than that of the graphite.

The aim of this work is to:

1. Utilise isothermal photo-DSC traces of cured resin samples in order to calculate the additional heating effect of the light source using non-isothermal models.
2. Determine the defining equations and parameters for the non-isothermal model. For the simple two-dimensional rectangular geometry considered these include the modified heat generation term, the material properties, the convection heat transfer coefficient as well as the initial and boundary conditions.
3. Calculate the temporal evolution of the temperature, the degree and rate of reaction and the glass transition temperature.

By performing the above mentioned modifications to the computations that have so far been published in the literature it is expected that the proposed phenomenological models will predict as closely as possible the curing behaviour of the VLC resins. Although the simulated specimens considered in the current work are based on a simple two dimensional geometry, the methods described herein are expected to be followed up by more complex, realistic models, which will impose less restrictions and assumptions on the derived solution. Hence, provided that the method described here is experimentally justified, it will be possible to investigate the curing performance of a particular composite for a given restoration cavity, as well as examine the thermal loading of the tooth tissues during the curing process. At the present time there is considerable interest in the utilization of extreme light intensities - very high and very low - in the photopolymerisation of dental composites. Thus the development of an accurate model of the photo-curing will greatly assist in the optimisation of the process.

2. Isothermal photo-DSC experimentation

The material under investigation was the dental VLC resin composite XRV-Herculite (Kerr UK Ltd., Peterborough, UK). This consists of dimethacrylate monomer mixture and silanated particulate glass filler with a camphoroquinone/amine photo-activated system. A DSC-7 apparatus (Perkin Elmer Corp., Norwalk, CT., USA) was used to perform isothermal photo-DSC measurements together with a VLC dental light curing unit (Luxor Light 4000, RFJ Electronics, Winsford, Cheshire, UK) with a blue light source (peak output at $\approx$470 nm), equipped with a fibre optic light guide. Photopolymerization was effected using a custom-made DSC cover, which allowed for the irradiation of the sample cell while at the same time providing the necessary thermal insulation within the furnace. In order to facilitate the accurate timing control of the light exposures, a high-speed electromagnetic shutter was used (Compur-Electronic GmbH, Köln, Germany), which was mounted on the exit window of the curing lamp. During the isothermal experiments, the DSC-7 computer supplied the necessary triggering pulses at predefined times to open and close the shutter, thus providing a full control over the sample irradiation sequence.

Six specimens of 15–20 mg of the composite were placed into standard aluminium pans and were carefully flattened, producing a layer of approximately 0.5 mm thick, in order to ensure isothermal conditions during cure. In order to avoid primary activation of the reaction, the preparation of the samples was performed at sub-ambient light levels.

The light exposure timing sequence followed for each isothermal measurement is shown with representative DSC traces in Fig. 1. Following the initial 40 s irradiation of a specimen (Signal 1), three additional measurements of equal duration were performed (Signals 2, 3 and 4) to obtain the average irradiant heating level so that it could be subtracted from the initial trace [5, 11, 12]. Finally, in order to determine the impulse response of the system which was necessary to deconvolve the isothermal data, each sample was exposed to a light pulse of 50 ms in duration (signal 5) (see Section 4 below, for deconvolution).

The cure of the composite was investigated at six temperatures from 25–50 °C at 5 degree intervals. As described elsewhere [6], the above outlined isothermal investigation together with additional dynamic DSC studies, yielded the necessary kinetic parameters for an autocatalysed phenomenological kinetic model commonly utilised to model the cure of light activated resin composites.

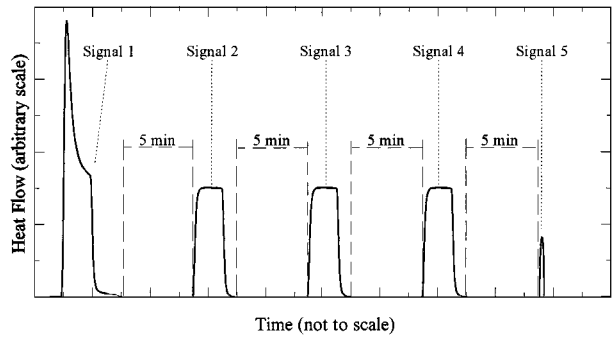

Figure 1 Isothermal photo-DSC timing sequence with typical signals obtained with the Herculite-XRV resin composite. Signal 1: reaction exotherm + irradiant exposure signal obtained from a 40 s irradiant exposure of the uncured specimen. Signals 2–4: irradiant heating signals obtained from a 40 s irradiant exposure of the cured specimen; Signal 5: measure of the response of the system, obtained from a 50 ms irradiant exposure.

3. Modification of the heat source term in the heat balance equation

In order to obtain a more accurate measure of the heat absorbed by the VLC composites, in addition to the isothermal reaction rate signals, the irradiant heating DSC measurements were also utilised. As shown in Fig. 1, the heat flow signals 2, 3 & 4, produced during the post-curing irradiations of the specimens provide this information. Fig. 2 illustrates the normalised averaged irradiant heating plots per temperature for the material XRV. It can be observed that these, unlike the reaction rate plots, do not follow a particular trend with temperature, since the reaction has been completed during the first light exposure (signal 1) and therefore can be regarded as a function of time only. The origin of the differences observed in these plots is discussed in the following section.

The two-dimensional, time dependent energy balance equation which provides the solution under non-isothermal conditions, can be written as follows [13]:

$$k\left(\frac{\partial^2 T}{\partial x^2}+\frac{\partial^2 T}{\partial y^2}\right)+g=\rho c_p\frac{\partial T(x,t)}{\partial t} \qquad (1)$$

where, T denotes the temperature, x, y the cartesian system coordinates, k the thermal conductivity of the material, g the heat source term, ρ the material density, c_p the specific heat and t the time.

So far, two configurations of the heat source term (g) have been presented in the literature related with non-isothermal transient analysis: the first considers the heat generation as the product of the exothermic reactions [5] (Equation 2a), whereas the second considers also the Beer-Lambert law in order to express the attenuation of the light energy as this passes through the material [7–9] (Equation 2b).

$$\begin{aligned} g(t,T)&=[R_p(t,T)H_{\max}]\rho \quad \text{(a)}\\ g(t,T,y)&=[R_p(t,T)H_{\max}]\exp(-by)\rho \quad \text{(b)}\end{aligned} \qquad (2)$$

where R_p is the reaction rate, $H_{\max}$ is the maximum heat of reaction, b is the attenuation coefficient encompassing the absorption and scattering effects taking place in the medium and y is the depth of light penetration.

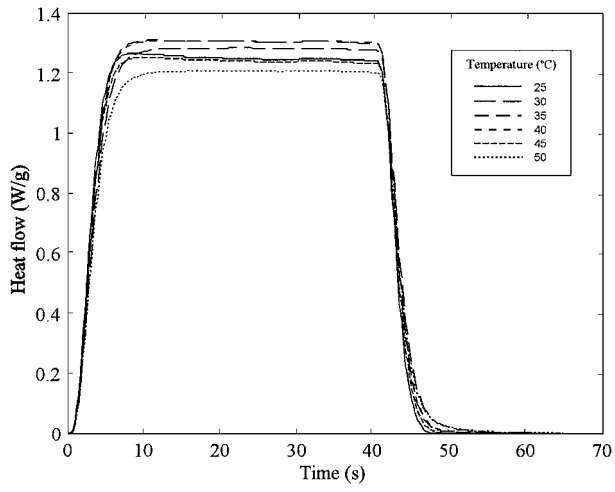

Figure 2 Average photo-DSC irradiant heating signals obtained at 25, 30, 35, 40, 45 and 50 °C for the Herculite-XRV resin composite at an intensity of 844 W m^{-2}.

However, g also represents the volumetric heat generation rate (in W · m^{-3}) arising from the absorption and scattering of light within the material and therefore can be calculated by multiplying the average irradiant heat flow signals from all temperatures by the density of the material. If the effect of the heat of cure is also to be investigated at the same time, the total heat source term should be equal to the sum of the individual heat source terms. As mentioned above, the additional heat source term is not a function of temperature, but instead it is only a function of time and therefore the calculations on the finite element model should incorporate the temporal variation of the heat flow signal. Equation 3 shows the proposed improvement in the heat generation term:

$$g(t,T,y)=[R_p(t,T)H_{\max}+B(t)]\exp(-by)\rho \qquad (3)$$

where $B(t)$ is the time dependent irradiant DSC trace.

Hence, in the subsequent calculations, Equation 3 is substituted in Equation 1. The rate of polymerization, R_p is provided by a phenomenological kinetic model, as expressed by the following ordinary differential equation (ODE) [5, 6]:

$$R_p\equiv\frac{\mathrm{d}a}{\mathrm{d}t}=ka^m(a_{\max}-a)^n \qquad (4)$$

where, a is the degree of reaction, $a_{\max}$ is the maximum attainable degree of reaction, m and n are fitting parameters and k is the rate constant following an Arrhenius temperature dependency:

$$k=k_0\exp\left(-\frac{E}{RT}\right) \qquad (5)$$

In the above equation, k_0 is the pre-exponential factor, E the activation energy and R the gas constant. Since the kinetic parameters for the phenomenological model (Equation 4) that are used in this study have been estimated from deconvolved isothermal data [6], it would be erroneous to use the irradiant heating data ($B(t)$) term in the heat source term calculations without prior deconvolution. The following section details the fundamental principles of the deconvolution process as well as a new method for its application to irradiant heating data.

4. Deconvolution of the irradiant heating data

Although DSC is a valuable method for monitoring enthalpic changes, the response time of the instrument, the thermal properties of the sample and the possible miscontact of the sample pan with the measuring furnace can all have a significant effect on the measurements. In other words, the "correct" signal that is produced by an exothermic reaction is "distorted" by any or all the above mentioned factors via a non-linear transformation termed convolution. This distorted signal can however be corrected if the opposite process is applied (deconvolution), provided that the impulse response of

the DSC is known for every sample studied. There are several techniques with which deconvolution can be applied to correct isothermal DSC data, using basic time, frequency or z-domain methods, optimised frequency or iterative methods [11] or even via the modified exponential function reconstruction (MEF) method [6].

The result of deconvolution of the irradiant heating data with the impulse response can be easier to anticipate than that obtained from the deconvolved isothermal reaction rate data [6, 11], where the original and the correct signals differ in terms of their shape, peak height or time at peak height. In this case we have a signal that varies abruptly only at the time intervals at which there is a light transition (Fig. 3a (Initial transition OFF-ON & Final transition ON-OFF)), whereas between the light transitions the signal reaches a plateau. Hence, since deconvolution mainly affects the portions of the signal which vary abruptly, the corrected signals should have steeper transitions and less changes to their plateau values. Indeed, the deconvolved signal in Fig. 3b proves the above assumption but also illustrates the weakness of the method to produce error-free signals. As it can be observed from Fig. 3b the initial portion of the signal

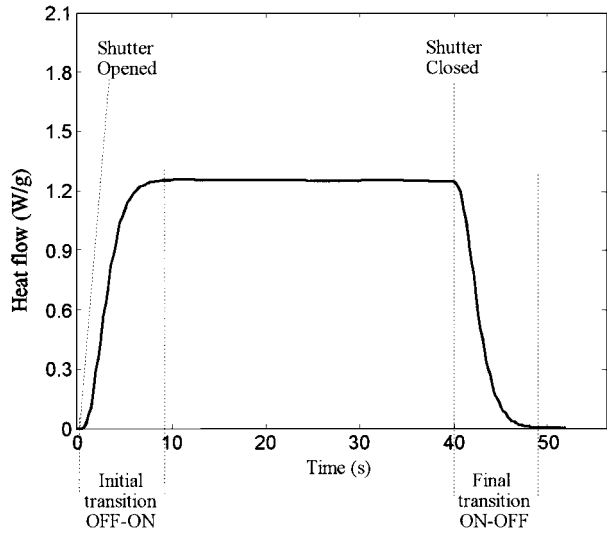

(a) Original irradiant heating signal

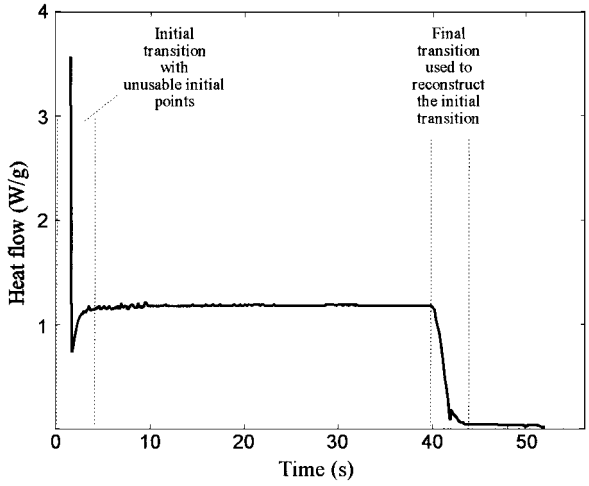

(b) Deconvolved irradiant heating signal of plot (a) with unusable initial points

Figure 3 Characteristics of the irradiant heating signals and deconvolution output without the initial point reconstruction procedure of an isothermal irradiant heating DSC signal obtained at 25 °C.

contains points that are unusable for further use. Similar problems with the initial points of the deconvolved isothermal reaction rate signals can also be observed in [6, 11] and are attributed to the sensitivity of this process to noise. However, in this case, in contrast with the reaction rate data, the initial part of the signal is not required to provide any *kinetic* parameters but instead it is essential to supply the necessary *initial increase of the heat flow signal* to the non-isothermal model.

The reconstruction of the lost initial points of the deconvolved irradiant heating signal in Figs 3b or 4a was based on a simple principle by using the inverted part of the final transition obtained at times $t \geq 40$ s. This was based on the fact that an OFF-ON light transition, observed at the beginning of an exposure should equal the ON-OFF transition observed at the end of the exposure, for both the original and the deconvolved data. Fig. 4b verifies that assumption for the original data by illustrating the initial (OFF-ON) transition plotted against the inverted final transition. Hence, if an ON-OFF transition of the deconvolved data is inverted and positioned at the problematic initial portion of the data, the signal can be restored. The reconstructed deconvolved curve is shown in Fig. 4c, against the original irradiant heating data obtained at 25 °C.

Applying convolution to the deconvolved signal yields a curve matching closely the original data, as illustrated in Fig. 4d. Similar results were obtained from the above mentioned transformations for all the temperatures tested, all verified by the excellent fit between the re-convolved deconvolved curve and the original irradiant heating data.

Following the procedure described above, all the irradiant heating plots (illustrated in Fig. 2) were deconvolved (Fig. 5a), averaged and smoothed thereafter (shown in Fig. 5b), providing the $B(t)$ term of Equation 3. From the comparative plot of Fig. 5a it can also be observed that the notable differences in the signal plateau levels that were observed prior to deconvolution process are now diminished, thus verifying that the method corrected the signals by also taking into account the differences between the individual samples. Hence, the differences in the plateau values observed in the plot can be regarded as a measure of the variance of the method.

5. Initial and boundary conditions

The solution(s) provided by Equation 1 are restricted to cases of internal heat transfer and do not fully describe heat transfer phenomena at the boundaries of the material during its cure. But once a resin composite is placed in a dental cavity, it is subjected to a number of different physical conditions across its boundaries. In order to determine the temperature distribution in such a case, it is essential to impose constraints (boundary conditions) on the solution of the heat balance equation, corresponding to the physical conditions existing at the boundaries of the medium and to the distribution of temperature at the origin of the time coordinate, $t = 0$ (initial conditions). These can be estimated by careful examination of the interfaces formed between the participating media.

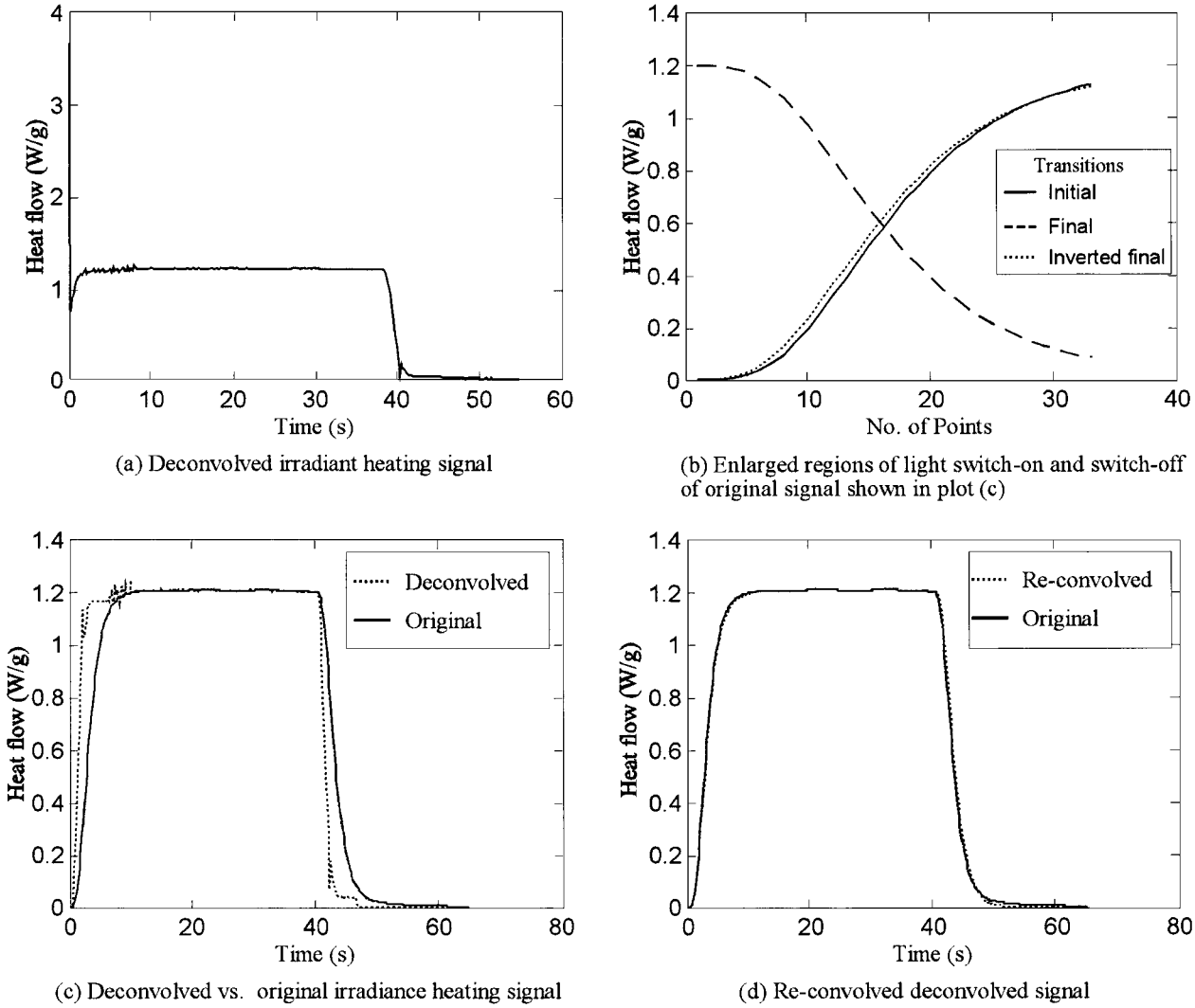

(a) Deconvolved irradiant heating signal

(b) Enlarged regions of light switch-on and switch-off of original signal shown in plot (c)

(c) Deconvolved vs. original irradiance heating signal

(d) Re-convolved deconvolved signal

Figure 4 Deconvolution and reconstruction procedure of isothermal irradiant heating DSC signal obtained at 45 °C.

To illustrate this procedure, a simple two-dimensional axisymmetric (around the y-axis) tooth-restoration model is considered in Fig. 6. In this, the air enclosed between the end tip of the fibre optic guide and the restoration surface exchanges heat with the heated composite through free convection whereas the bottom and the side walls of the composite conduct heat through the tooth tissue. Since this is only an approximate model and this work is not concerned with the thermal loading of the oral tissues, the bottom and side surfaces of the composite can be assumed to have a constant temperature (T_b), maintained by the blood micro-circulation in the pulp and the surrounding tissues. Starting from these boundaries, the prescribed temperature boundary conditions as well as the initial conditions (T_i) can be expressed as follows:

$$T(x,y,t) = T_b \quad 0 \le x \le x_1 \;\; y = y_1 \;\; t \ge 0 \qquad \text{(a)}$$

$$T(x,y,t) = T_b \quad x = x_1 \;\; 0 \le y \le y_1 \;\; t \le 0 \qquad \text{(b)}$$

$$T(x,y,t) = T_i \quad 0 \le x \le x_1 \;\; 0 \le y \le y_1 \;\; t = 0 \qquad \text{(c)} \tag{6}$$

The top surface of the composite is subjected to convection boundary conditions, therefore the convection heat flux at these will equal the conductive heat flux:

$$h(T_A - T(x,y,t)) = -k\frac{\partial T(x,y,t)}{\partial y}$$
$$0 \le x \le x_1 \;\; y = 0 \;\; t > 0 \tag{7}$$

where h is the heat transfer coefficient and T_A is the temperature of air.

The convection heat transfer coefficient (h), which indicates the efficiency of heat dissipation at the composite-air interface, can be calculated using dimensional analysis parameters. This method differs from other approaches in that it does not yield equations but instead it combines several variables into dimensionless groups, such as the Nusselt number (Nu), which expresses the level of the temperature gradients existing at a surface which comes in contact with the air. These parameters facilitate the interpretation and extend the range of application of experimental data [13]. For two horizontal surfaces having a distance L, separated with air with thermal conductivity k_{air}, h is given by Equation 8:

$$h = \frac{NuL}{k_{air}} \tag{8}$$

An empirical equation, valid for cases where there are two parallel surfaces from which the bottom one is

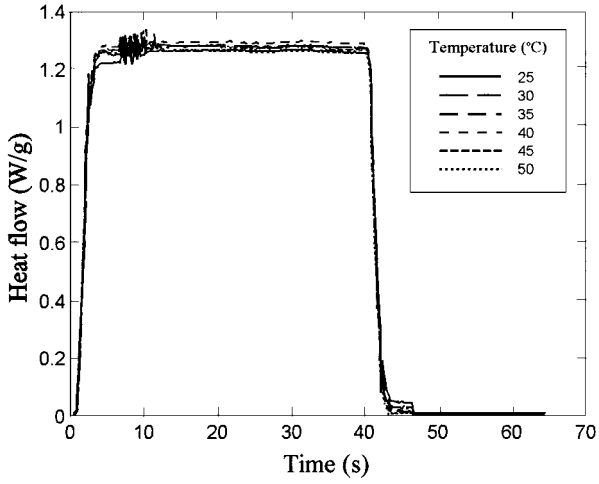

(a) Deconvolved irradiant heating signals for each isothermal temperature tested

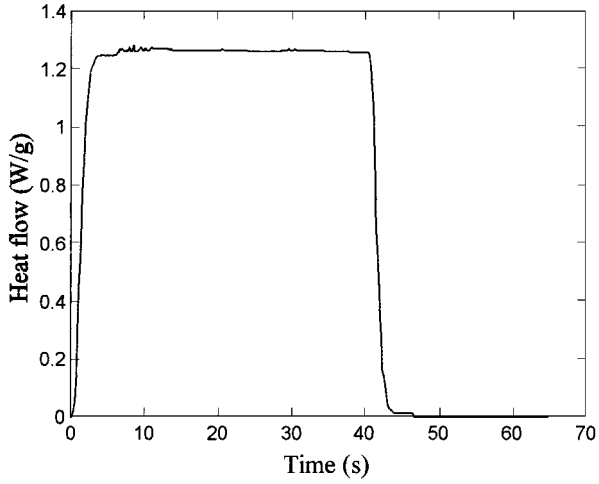

(b) Smoothed deconvolved signal produced from averaging the plots in (a)

Figure 5 Deconvolved photo-DSC irradiant heating signals of Fig. 2 and averaged deconvolved irradiant data; $B(t)$.

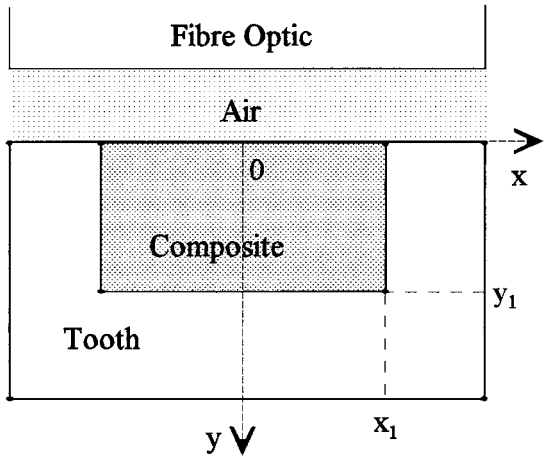

Figure 6 Approximate two-dimensional, axissymetric tooth-restoration geometry.

heated (i.e. the composite) can be used to calculate the Nusselt number [14] as follows:

$$Nu = 1 + 1.44\left[1 - \frac{1708}{Ra}\right]^{*} + \left[\left(\frac{Ra}{5830}\right)^{1/3} - 1\right]^{*} \quad (9)$$

where the notation $[\ ]^{*}$ indicates that if the quantity inside the bracket is negative, the quantity is to be taken as zero. Ra is the Rayleigh number, which is the defining parameter for instability in turbulent free convection flows. This is given by:

$$Ra = \frac{c_p g \beta_{\text{air}} (T - T_{\text{air}}) L^3 \rho_{\text{air}}^2}{k_{\text{air}} \mu_{\text{air}}} \quad (10)$$

where g is the acceleration due to gravity, β_{air} $(=((T + T_{\text{air}})/2)^{-1}$ K) is the compressibility of air, T is the temperature of the heated surface (i.e. the composite) and μ_{air} the viscosity of air.

In cases where a more complex geometry exists at the interface where convection takes place, the above calculations are not valid, since they have been calculated strictly for flat parallel surfaces. However, numerical methods that simulate the fluid (air) flow can be utilised to give an accurate prediction on the convection coefficient, even when complex geometries are involved [13].

The models considered in this analysis were taken to have a plane rectangular geometry, with dimensions 2×2 mm. The top surface of the composite which comes in contact with the air was assigned a convection coefficient of $h = 4.18$ (W m^{-1} K^{-1}), calculated using Equations 9 and 10 for a temperature difference between the air and the composite of 20 degrees and a distance of 6 mm between the composite surface and the fibre optic. Therefore, Equation 9 predicts a very low convection coefficient equally indicating that the interface has a negligible heat dissipation efficiency.

In addition, the bottom and the sides of the rectangular model were assigned a constant temperature of $T_{\text{b}} = 309.15$ K (36 °C) throughout the analysis, simulating coarsely the conduction effect of the tooth tissue surrounding the material. Finally, an initial condition of $T_{\text{i}} = 309.15$ K was assigned to all the remaining nodes of the model.

6. Mesh density and time step determination

The major difficulties an analyst faces when implementing a finite element/difference analysis problem are usually associated with the appropriate discretisation of the spatial and of the time domain if the analysis is transient. One method, commonly used to determine the optimum element size or time step for the problem, requires to obtain a series of solutions by varying the element size and/or time step and observing the variation in the solution [15]. Since the computational effort involved in this can be high, the so-called dimensional analysis can be utilized offering significant advantages over the traditional approach, since the solution is calculated over relative distances rather than at fixed points within the model geometry. A brief example of this type of analysis was shown in the previous Section where the calculation of the heat transfer coefficient (h) was based on the dimensionless parameters Nu and Ra. In order to implement a dimensional analysis the heat balance equation is written in a dimensionless form by modifying appropriately the various constituent parameters. However, these dimensionless parameters are not valid

in cases where irregular geometries are considered and their estimation at particular locations requires the solution of the appropriate differential equations describing the phenomenon. In other words, the method becomes too involved to be practical [13].

For the purposes of this investigation, where the geometrical models under consideration are simple, a dimensional analysis would be adequate to achieve a solution. It was decided however to effect a solution by using the first approach, as in the future, our work will contain geometrical models corresponding to the complex tooth restoration geometries commonly encountered in the clinical practice. Hence, the heat balance equation considered was that of the form of Equation 1, in conjunction with the Crank-Nicolson time integration scheme [15].

The analysis for this and all subsequent steps in this investigation was performed using the commercial finite element program ANSYS (Swanson Analysis Systems Inc., PA, USA), running on a Unix-based, Sun UltraEnterprise 2000 computer (Sun Microsystems, CA, USA). Using as an input to the kinetic model the kinetic parameters provided by Maffezzoli *et al.* [5] on a one-dimensional model (length = 1 mm), the element size as a proportion of the model length was varied from a ratio of 1/80 to 1/3, whilst the time step was kept constant at 1 s. The observed maximum temperatures were subtracted from the temperature obtained using the smallest element size (1/80) which should be very close to the theoretical temperature. Fig. 7 illustrates the relationship between the percentage difference in the maximum temperature observed versus the relative element size. From this, a relative element size of 1/6 was selected for the remainder of the analysis, considering an error of less than 0.02% as acceptable. It should be noted here that, although smaller element sizes are certainly preferable in terms of accuracy, the execution time increases considerably from several minutes to several hours, with no considerable improvement in the accuracy of the solution.

In the above analysis, the time step used from the ANSYS finite element solver was equal to that used by the solver performing the integration on the phenomenological models' reaction rate expression. This was necessary since, it would be meaningless to advance the solution of the ordinary differential equation (ODE) (Equation 4) at a different rate than that solved by the finite element solver. The ODE solver implemented in ANSYS was a fixed-step, fourth order Runge-Kutta algorithm.

A determination of the optimum time step for the finite element solver alone could introduce errors in the analysis, since this may be excessive for the Runge-Kutta algorithm and cause it to predict erroneous values for the degree of reaction. Therefore, an additional investigation was performed to determine the optimum time step for the ODE solver. This consisted of series of computations, in which each Runge-Kutta increment was tested against a range of finite element solver increments. In every case examined, the number of iterations of the ODE solver was such that the ODE time step would equal the finite element solver increment. Fig. 8 illustrates the maximum temperature variations, obtained using a range of ODE solver time increments (from 0.001 to 0.2 s) with variable finite element increments (FEI = 0.2 to 1.4 s). Identical solutions were obtained for all the ODE solver increments tested. However, these also demonstrate that the accuracy of the solution depends heavily on the value of the increment of the finite element solver.

From the above it was postulated that an ODE solver time increment of 0.2 s was acceptable, whereas the same can be assumed for the time increment of the finite element solver, provided that the solution does not vary considerably for smaller values (i.e. FEI, ODE <0.2 s). To verify this, additional tests were conducted whereby the ODE/FE increments were equally varied from 0.2 to 0.01 seconds. Fig. 9 illustrates the temperature variations observed from all tests, demonstrating

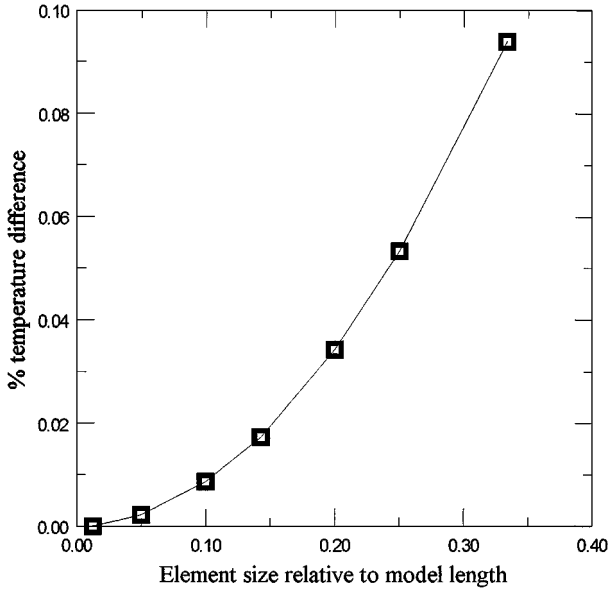

Figure 7 Percentage variation of the calculated temperature difference in relation to the smallest mesh as a function of mesh density.

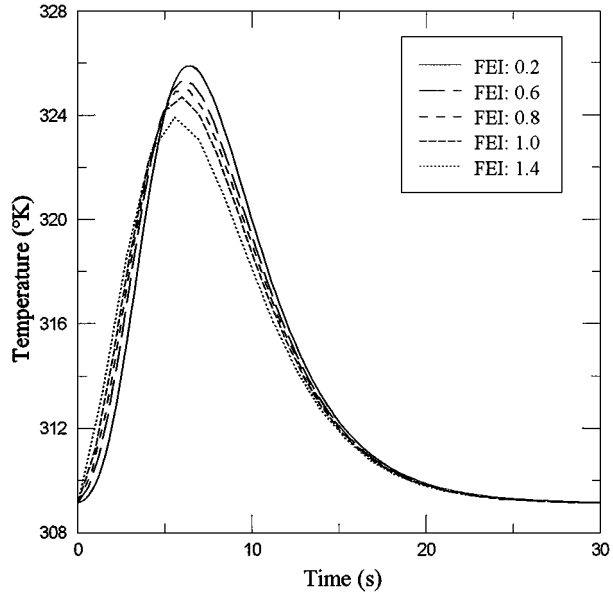

Figure 8 Variation of predicted temperature with ODE solver time increments (0.001, 0.01, 0.1 and 0.2 s) and variable finite element solver time increments (0.2, 0.6, 0.8, 1.0, 1.4 s).

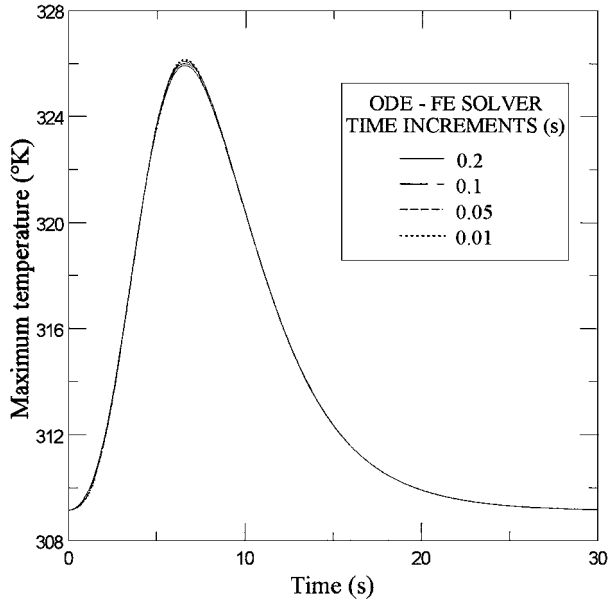

Figure 9 Variation of predicted temperature obtained using common variable ODE/Finite Element solver time Increments (0.2, 0.1, 0.05 & 0.01 s).

that for time increments smaller than 0.2 seconds only marginal improvement in the accuracy of the solution was observed (0.01% difference).

7. Material properties

7.1. Specific Heat

Specific heat measurements of VLC dental composite resins have been performed mainly during the past decade by means of two techniques: DSC [16] and Differential Thermal Analysis (DTA) [17]. Despite the importance of this parameter, reports on its estimation for newer types of VLC dental materials are very limited. Specific heat calculations have become trivial using DSC instruments operating in scanning mode [18]. The measurements were performed using a power compensated DSC system (Perkin Elmer Corp., Norwalk, CT., USA), equipped with a water cooling accessory to facilitate measurements starting at the ambient temperature range.

Multiple specimens of material were produced, positioned into weight-matched aluminium pans and cured for 40 s at ambient conditions (23 °C, 64 ± 1% RH) using a Luxor light source. All specimens and aluminium pans were weighted to a precision of ±0.01 mg (typically ∼20 mg). Following curing, the specimens were sealed with weight-matched lids and kept for at least 24 hours in opaque containers prior to measurement.

Temperature calibration was obtained by observing the melting transition of reference materials (of both Indium and zinc), using dry nitrogen as purging gas (flow rate: 20 mL/min) and 10 degrees/min heating rate. Following this, heat flow calibration was performed, using a synthetic sapphire disk (0.3 mm × 3 mm diameter) (Perkin Elmer, Part no: 0219–1269) and scanning at the same heating rate, at a temperature interval from 25 to 60 °C. At the start of each run, the specimen was held at the starting temperature for 5 min in order to reach equilibrium. A calibration constant was determined from the ratio of published specific heat capacity for sapphire [18] vs the experimental values and this was found to be 0.971. This constant was then applied as a correction factor through the DSC software controlling the apparatus.

Prior to each specific heat determination, a dynamic run was performed with only the aluminium specimen holders (plus lids) placed in each measuring cell (sample and reference) of the DSC apparatus. Consequently, the same specimen pan and lid used for the irradiant heating measurement was used to hold and seal each material sample. At the end of each dynamic run, the Perkin Elmer DSC software automatically subtracted the mW reading obtained from the irradiant heating data from the specimen's endothermic response in order to obtain the true power reading used to calculate the specific heat (as required from the ASTM procedure). The resulting data in (mW) were then divided by the sample weight (mg) and the scanning rate (°C/sec) to provide the measured specific heat of the specimen in $J(g^{\circ}C)^{-1}$.

TABLE I Material properties and finite element model parameters used

Parameter	Value	References
b	0.00028 (m^{-1})	[7]
c_p	938.8 ($J{\cdot}Kg^{-1}{\cdot}K^{-1}$)	
h	4.18 ($W{\cdot}m^{-2}{\cdot}K^{-1}$)	
k	0.2941 ($W{\cdot}m^{-1}{\cdot}K^{-1}$)	[19]
L	0.006 (m)	
T_i	309.15 (K)	
T_b	309.15 (K)	
ρ	2094.11 ($Kg{\cdot}m^{-3}$)	[19]

7.2. Thermal conductivity & density

The thermal conductivity and density values were taken from a study performed on cured specimens of the material under investigation [19]. These were derived from measurements of thermal diffusivity using a method developed by Watts and Smith [20].

Table I summarizes the above as well as the previously extracted parameters that were used to perform the finite element simulation.

8. Model implementation - Cases examined

The two-dimensional exploratory models that will be presented in this Section were developed in order to enhance our understanding on the effect of the different cure assumptions (imposed via the heat generation term) on the cure characteristics of the three materials investigated. Three cases were examined, with each considering:

Case 1 - homogeneous absorption of light along the depth of the composite (heat generation due to the polymerization reaction only). Heat generation term provided by Equation 2(a)

Case 2 - exponential decay of the light penetration along the specimen thickness (heat generation due to the exothermic reaction only). Heat generation term provided by Equation 2(b)

Case 3 - exponential decay of the light penetration along the specimen thickness, including the heat generated by the combined effect of the exothermic reactions and the irradiant heat generation arising from the curing unit. Heat generation term provided by Equation 3

The design of the models was such that it imposed several assumptions with regards to the material's behaviour and the conditions existing during cure. These were:

1. Homogeneous and temperature independent material properties
2. No flow of material (mass transport) during processing
3. No radiation heat exchange mechanism between the heating surface of the composite and the fibre optic
4. No shrinkage effects were considered
5. No residual - dark polymerization effects were modelled.

The material properties of the composite were assumed to be homogeneous and temperature independent, as is widely accepted by several researchers [21–23]. Flow effects are believed to be negligible during light exposure, since gelation occurs rapidly after the onset of polymerization. Consequently no significant density changes within the bulk of the composite are expected to occur during polymerization [24].

The radiation heat transfer mechanism was not considered in any of the following models, including the ones described in subsequent sections, due to the lack of data referring to the emissivity and absorptivity properties of composite resins. The mechanism of radiative heat transfer during the cure of VLC composites, should occur between the heated surface of the composite and the fibre optic. This should not influence the results of this study, provided that the surface temperature of the composite during the cure does not attain excessively high values. In the latter case this mechanism may prove to assist significantly the heat dissipation from the composite.

Shrinkage was not considered as a variable in these analyses as this was beyond the scope of this research. Microscopic gap formation within the dental cavity is expected to affect to some extent the heat transfer mechanism between the curing composite and the adjacent tooth tissues.

Thermal analysis kinetic models impose an assumption on the ceasation of the reaction. More specifically, there is evidence to support that dark polymerization reaction occurs for some period in photopolymer systems following initial cure, as free-radicals still exist for at least a further 24 hours [25]. The rate of these reactions is much reduced compared with that observed during the light exposure, as it is dictated by the ability of the free radicals to diffuse and find unreacted monomer in a dense cross-linked chain network. Despite the above mentioned problem, thermal analysis kinetic models have demonstrated their potential to reveal significant features of the cure mechanisms in non-isothermal conditions.

9. Results and discussion

Figs 10–12 display the results (temperature, degree of reaction and glass transition temperature) obtained from the finite element solution of the composites for each case considered, for the material Herculite-XRV.

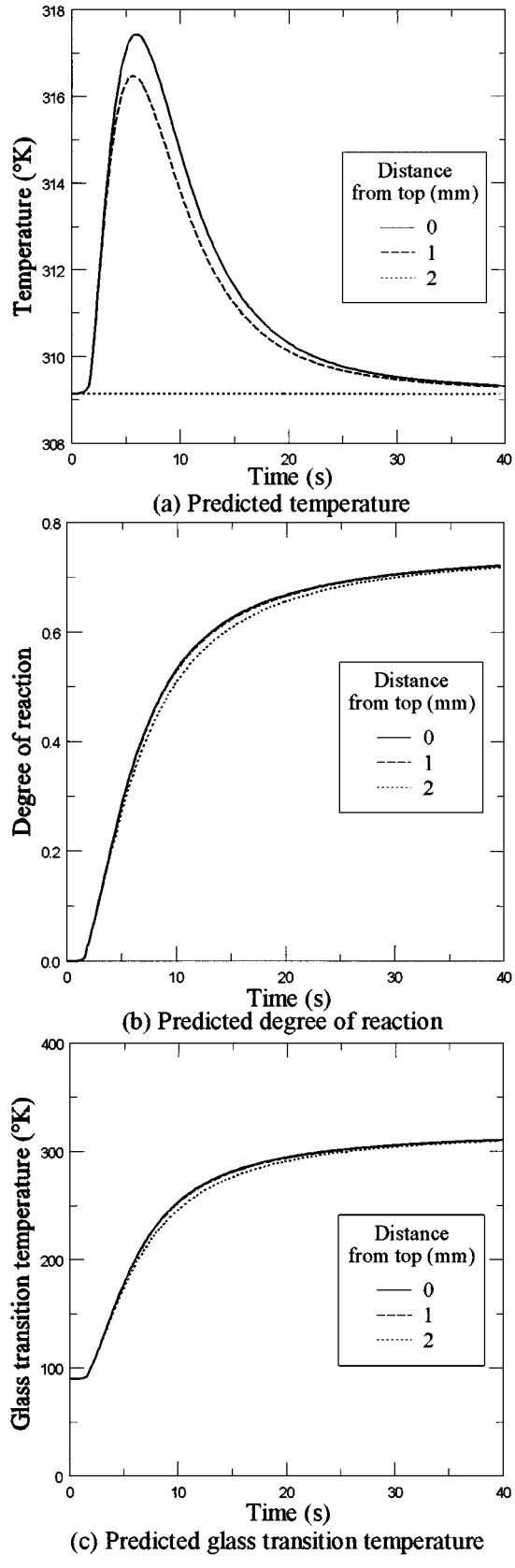

Figure 10 Results from a non-isothermal 2-D transient simulation considering a plane rectangular geometry of the VLC resin composite Herculite-XRV - Case 1.

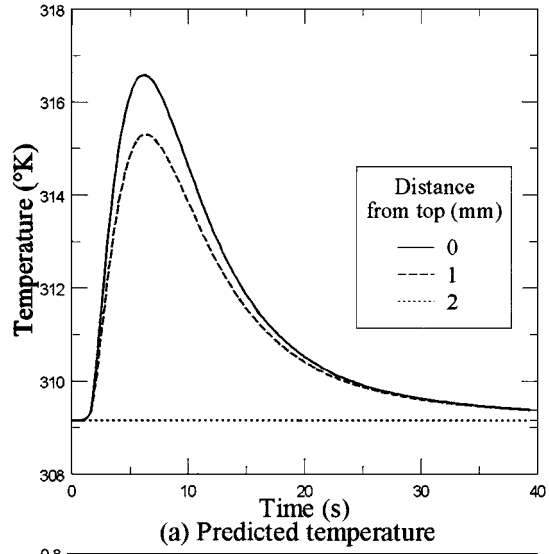

(a) Predicted temperature

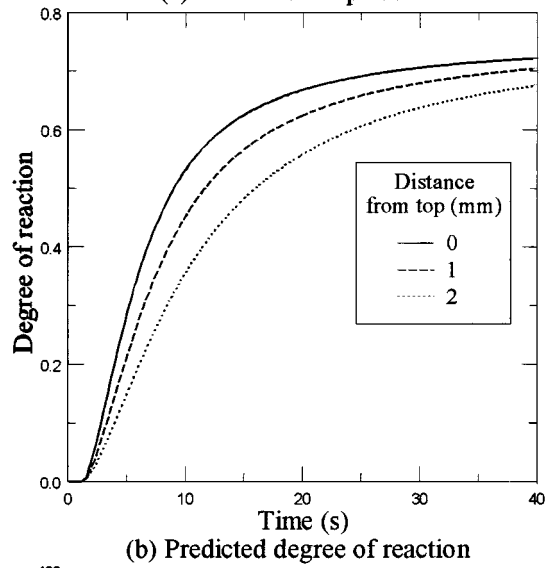

(b) Predicted degree of reaction

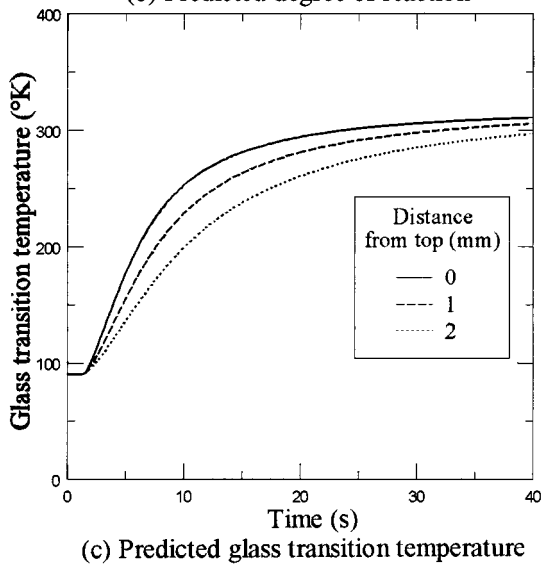

(c) Predicted glass transition temperature

Figure 11 Results from a non-isothermal 2-D transient simulation considering a plane rectangular geometry of the VLC resin composite Herculite-XRV - Case 2.

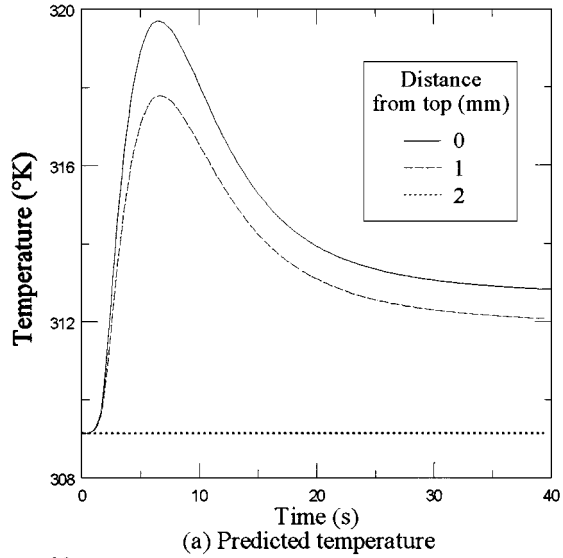

(a) Predicted temperature

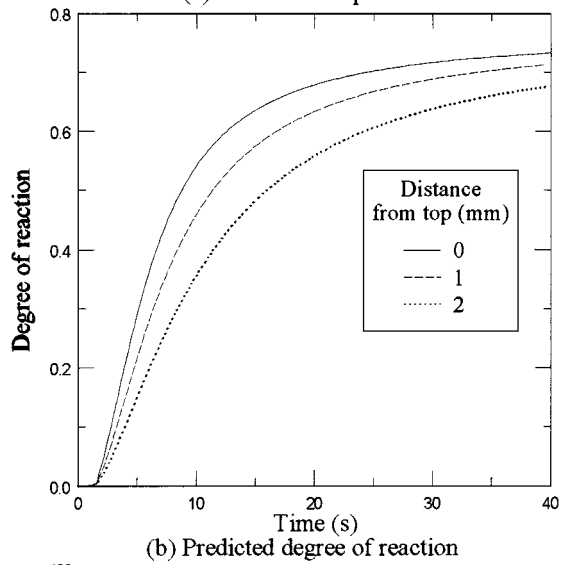

(b) Predicted degree of reaction

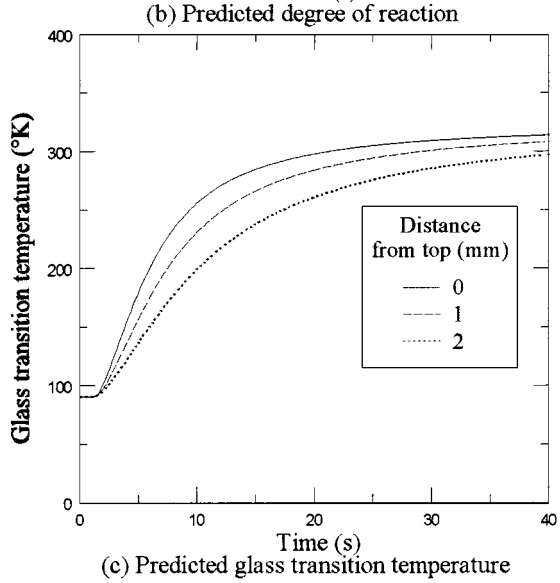

(c) Predicted glass transition temperature

Figure 12 Results from a non-isothermal 2-D transient simulation considering a plane rectangular geometry of the VLC resin composite Herculite-XRV - Case 3.

The glass transition temperature was calculated via a simple linear relationship with the degree of reaction [6]. In order to facilitate a direct comparison between the three different cases considered, Table II presents the maximum values obtained from the analysis of the maximum temperature (T_{max}), the maximum reaction rate ($R_{P\,max}$), the degree of reaction (α_{max}) and the final glass transition temperature ($T_{g\,final}$), at the top and the core of the model. Also quoted are the times at which these maximum values were observed.

By observing the temperature plots from all the cases examined, it can be derived that the exothermic

TABLE II Maximum parameter values observed at the surface and the core of the model (Results from Cases 1, 2 & 3)

	Values at the surface of the model			Values at the core of the model		
Parameter	Case 1	Case 2	Case 3	Case 1	Case 2	Case 3
T_{max} (K)	317.4	316.6	319.7	316.5	315.3	317.8
Time (s)	6	6.2	6.6	5.6	6.4	6.6
Rate (s^{-1})	0.0887	0.0883	0.0898	0.886	0.0669	0.0681
Time (s)	3.2	3.2	3.4	3.2	3.8	4
Degree	0.7224	0.7226	0.7322	0.7219	0.7052	0.7131
$T_{g\,final}$	310.9	311	313.9	310.8	305.7	308.1

polymerization reaction is mainly responsible not only for the overall profile of the temperature variation with time but also for the magnitude of the temperature rises. Since the only mechanism of heat dissipation in the material is through convection at the surface, the heat is generated at higher rates than it can be transferred to the air. As a consequence, the temperature rises follow closely the reaction rate profiles. The introduction of the exponential attenuation of the heat generation term (Case 2), as expected, resulted in an overall temperature decrease throughout the volume of the composite. By incorporating the irradiant heat term in the calculation (Case 3), the temperature profile was affected in several ways. Firstly, the peak value attained was greater by 3.1 degrees compared with the Case 2 result and secondly, the rate of change of the plot at the portion following the peak is significantly lower than the previous calculations. This is due to the contribution of the irradiant heat generation term during the exposure which continuously increases the temperature field whilst the reaction rate almost ceases to produce noticeable temperature differences.

The degree of reaction plots indicate more clearly the effect of the exponential attenuation of light absorption than the corresponding temperature plots. As it can be observed in Case 1, the degrees of reaction at the surface and the core are comparable, whereas in Case 2 their differences are pronounced. Case 3 is particularly interesting in the sense that it reveals that the increased temperature levels do not correspond necessarily with pronounced changes in the degree of cure. This can be explained from the fact that the average temperature increase from the heating effect of the light is in the order of 3 degrees K. By taking into account the behaviour of the isothermal kinetic model, one can derive that the degree and rate of reaction for the given temperature change will only be slightly elevated.

The glass transition temperature plots display a similar behaviour with the corresponding degree of reaction plots. This was anticipated since the former parameter is calculated from the simple linear relationship with the degree of cure [5, 6].

Although the figures displayed above reveal in full the transient variation of the calculated parameters, Table II is more explanatory in the sense that differences between each case, as well as between materials, can easily be depicted. Starting from the maximum temperature (T_{max}), Table II shows that Case 3 produced the highest values; an increase of approximately 3 degrees was observed above the temperatures obtained in Case 2. Accordingly, the temperature increases at the core due to the irradiant heating effect are between 1.5 to 2.5 degrees K.

An interesting decrease in the maximum temperature at the top is observed between Cases 1 and 2, where it can also be noticed that the inclusion of the exponential attenuation of the light absorption effects (Case 2) reduced the reaction rate. This implies that in Case 2, lower temperatures were observed underneath the surface, as indeed the temperature value at the core indicates (see Table II, compare T_{max} Cases 1 & 2). Therefore, the heat flow from nearby nodes towards the surface nodes was not sufficiently high to enhance the rate of reaction at the surface (thus explaining the reduced reaction rates observed there). Certainly, the effect of the attenuation of light is more pronounced with increasing depth and therefore the degree of reaction differences increase with depth. Case 3 also reveals that the reaction rate was slightly enhanced by the inclusion of the heating effect, in both the top and the core of the material.

One drawback of the models considered in this work is that the calculation of the reaction rate at the side and bottom boundary nodes does not depend on the temperatures produced by neighbouring nodes, or on the exotherm produced at these locations. Instead, the reaction rate is calculated based upon the prescribed boundary condition (309.15 K). This shows that such models do not entirely represent the physical situation since the tooth tissue conducts heat generated from the microcirculation in the pulp and therefore its temperature is not constrained.

Acknowledgements

The authors wish to acknowledge the help of Dr. Wayne Cook of Monash University, Australia for his advice during the early stages of this work and the late Mr. R. Turner of Kerr UK Ltd for the kind supply of materials.

References

1. J. F. STEVENSON, *Polym. Eng. Sci.* **26** (1986) 746.
2. W. D. COOK, *Polymer* **33** (1992) 600.
3. P. W. K. LAM, H. P. PLAUMANN and T. TRAN, *J. Appl. Polym. Sci.* **41** (1990) 3043.
4. J. M. KENNY and A. TRIVISANO, *Polym. Eng. Sci.* **31** (1991) 1426.
5. A. MAFFEZZOLI, A. DELLAPIETRA, S. RENGO, L. NICOLAIS and G. VALLETTA, *Biomaterials* **15** (1994) 1221.
6. D. PANANAKIS and D. C. WATTS, *Polymer*, submitted.
7. A. MAFFEZZOLI, R. TERZI and L. NICOLAIS, *J. Mater. Sci.: Mater. Med.* **6** (1995) 161.
8. L. FLACH and R. P. CHARTOFF, *Polym. Eng. Sci.* **35** (1995) 483.

9. *Idem.*, *ibid.* **35** (1995) 493.
10. E. FISHER, W. KUNZE and B. STAPP, Perkin Elmer Analysentechniche Berichte (Report on Analysis Techniques) 1988, p. 1.
11. D. PANANAKIS and E. W. ABEL, *Thermochim. Acta* **315** (1998) 107.
12. J. VAIDYANATHAN and T. K. VAIDYANATHAN, *J. Mater. Sci.: Mater. Med.* **3** (1992) 19.
13. F. KREITH and M. BOHN, "Principles of Heat Transfer," 5th ed. (West Publishing Company, St. Paul, MN., 1995) p. 80.
14. K. G. T. HOLLANDS, G. D. RAITHBY and L. KONICEK, *Int. J. Heat Mass Tran.* **18** (1975) 879.
15. O. C. ZIENKIEWICZ and R. L. TAYLOR, "The Finite Element Method, Vol. 2: Solid and Fluid Mechanics Dynamics and Non-Linearity," 4th ed. (McGraw-Hill, London, 1991) pp. 269 and 352.
16. J. F. MCCABE and H. J. WILSON, *J. Oral Rehabil.* **7** (1980) 103.
17. C. H. LLOYD, *Biomaterials* **2** (1981) 179.
18. American Society For Testing and Materials, in Annual Book of ASTM Standards: E 1269–95.
19. G. TOWORFE, PhD thesis, University of Manchester, Manchester, UK, 1998.
20. D. C. WATTS and R. SMITH, *J. Dent. Res.* **60** (1980) 1972.
21. J. H. P. DEVREE, M. PETERS and A. J. M. PLASSCHAERT, *ibid.* **63** (1984) 1217.
22. T. A. M. SPIERINGS, F. BOSMAN, M. PETERS and A. J. M. PLASSCHAERT, *Dent. Mater.* **4** (1988) 51.
23. M. M. WINKLER, T. R. KATONA and N. H. PAYDAR, *J. Dent. Res.* **75** (1996) 1477.
24. A. VERSLUIS, W. H. DOUGLAS, M. CROSS and R. L. SAKAGUCHI, *ibid.* **75** (1996) 871.
25. D. C. WATTS, in "Dental and Medical Materials," Vol. 14, edited by D. F. Williams (Weinheim, FRG: VCH Verlagsgesellschaft mbH., 1992) Ch. 6, p. 209. Materials Science and Technology: A Comprehensive Treatment, edited by R. W. Cahn, P. Haasen and E. J. Kramer.

Received 30 July 1999
and accepted 14 March 2000